

First measurements of absolute branching fractions of the Ξ_c^+ baryon at Belle

Y. B. Li,⁷¹ C. P. Shen,¹⁰ I. Adachi,^{17, 14} J. K. Ahn,³⁸ H. Aihara,⁸⁸ S. Al Said,^{82, 35} D. M. Asner,³ H. Atmacan,⁷⁸ T. Aushev,⁵⁶ R. Ayad,⁸² V. Babu,⁸ A. M. Bakich,⁸¹ Y. Ban,⁷¹ V. Bansal,⁶⁹ P. Behera,²⁴ C. Belenõ,¹³ M. Berger,⁷⁹ V. Bhardwaj,²¹ B. Bhuyan,²² T. Bilka,⁵ J. Biswal,³² A. Bobrov,^{4, 67} A. Bozek,⁶⁴ M. Bračko,^{50, 32} T. E. Browder,¹⁶ M. Campajola,^{29, 59} L. Cao,³³ D. Červenkov,⁵ V. Chekelian,⁵¹ A. Chen,⁶¹ B. G. Cheon,¹⁵ K. Chilikin,⁴³ H. E. Cho,¹⁵ K. Cho,³⁷ Y. Choi,⁸⁰ S. Choudhury,²³ D. Cinabro,⁹² S. Cunliffe,⁸ S. Di Carlo,⁴¹ Z. Doležal,⁵ D. Dossett,⁵² S. Eidelman,^{4, 67, 43} D. Epifanov,^{4, 67} J. E. Fast,⁶⁹ T. Ferber,⁸ B. G. Fulsom,⁶⁹ R. Garg,⁷⁰ V. Gaur,⁹¹ N. Gabyshev,^{4, 67} A. Garmash,^{4, 67} A. Giri,²³ P. Goldenzweig,³³ B. Grube,⁸⁴ O. Grzymkowska,⁶⁴ J. Haba,^{17, 14} T. Hara,^{17, 14} K. Hayasaka,⁶⁶ H. Hayashii,⁶⁰ W.-S. Hou,⁶³ T. Iijima,^{58, 57} K. Inami,⁵⁷ G. Inguglia,²⁷ A. Ishikawa,¹⁷ M. Iwasaki,⁶⁸ Y. Iwasaki,¹⁷ W. W. Jacobs,²⁵ S. Jia,² Y. Jin,⁸⁸ D. Joffe,³⁴ K. K. Joo,⁶ A. B. Kaliyar,²⁴ G. Karyan,⁸ Y. Kato,⁵⁷ T. Kawasaki,³⁶ H. Kichimi,¹⁷ C. H. Kim,¹⁵ D. Y. Kim,⁷⁷ H. J. Kim,⁴⁰ K. T. Kim,³⁸ S. H. Kim,¹⁵ K. Kinoshita,⁷ P. Kodyš,⁵ S. Korpar,^{50, 32} D. Kotchetkov,¹⁶ P. Križan,^{45, 32} R. Kroeger,⁵³ P. Krokovny,^{4, 67} T. Kuhr,⁴⁶ R. Kulasiri,³⁴ A. Kuzmin,^{4, 67} Y.-J. Kwon,⁹⁴ K. Lalwani,⁴⁸ J. S. Lange,¹¹ I. S. Lee,¹⁵ J. K. Lee,⁷⁵ J. Y. Lee,⁷⁵ S. C. Lee,⁴⁰ C. H. Li,⁴⁴ L. K. Li,²⁶ L. Li Gioi,⁵¹ J. Libby,²⁴ K. Lieret,⁴⁶ D. Liventsev,^{91, 17} P.-C. Lu,⁶³ J. MacNaughton,⁵⁴ M. Masuda,⁸⁷ T. Matsuda,⁵⁴ D. Matvienko,^{4, 67, 43} M. Merola,^{29, 59} K. Miyabayashi,⁶⁰ H. Miyata,⁶⁶ R. Mizuk,^{43, 55, 56} G. B. Mohanty,⁸³ T. J. Moon,⁷⁵ R. Mussa,³⁰ M. Nakao,^{17, 14} K. J. Nath,²² M. Nayak,^{92, 17} M. Niiyama,³⁹ N. K. Nisar,⁷² S. Nishida,^{17, 14} K. Nishimura,¹⁶ S. Ogawa,⁸⁵ H. Ono,^{65, 66} Y. Onuki,⁸⁸ P. Pakhlov,^{43, 55} G. Pakhlova,^{43, 56} B. Pal,³ S. Pardi,²⁹ H. Park,⁴⁰ S.-H. Park,⁹⁴ S. Patra,²¹ S. Paul,⁸⁴ T. K. Pedlar,⁴⁷ R. Pestotnik,³² L. E. Piilonen,⁹¹ V. Popov,^{43, 56} E. Prencipe,¹⁹ M. Ritter,⁴⁶ A. Rostomyan,⁸ G. Russo,⁵⁹ D. Sahoo,⁸³ Y. Sakai,^{17, 14} M. Salehi,^{49, 46} L. Santelj,¹⁷ T. Sanuki,⁸⁶ V. Savinov,⁷² O. Schneider,⁴² G. Schnell,^{1, 20} J. Schueler,¹⁶ C. Schwanda,²⁷ Y. Seino,⁶⁶ K. Senyo,⁹³ M. E. Sevior,⁵² V. Shebalin,¹⁶ J.-G. Shiu,⁶³ B. Shwartz,^{4, 67} F. Simon,⁵¹ A. Sokolov,²⁸ E. Solovieva,⁴³ M. Staric,³² Z. S. Stottler,⁹¹ J. F. Strube,⁶⁹ M. Sumihama,¹² T. Sumiyoshi,⁹⁰ M. Takizawa,^{76, 18, 73} U. Tamponi,³⁰ K. Tanida,³¹ F. Tenchini,⁸ M. Uchida,⁸⁹ T. Uglov,^{43, 56} Y. Unno,¹⁵ S. Uno,^{17, 14} Y. Ushiroda,^{17, 14} S. E. Vahsen,¹⁶ R. Van Tonder,³³ G. Varner,¹⁶ A. Vinokurova,^{4, 67} B. Wang,⁵¹ C. H. Wang,⁶² M.-Z. Wang,⁶³ P. Wang,²⁶ S. Watanuki,⁸⁶ E. Won,³⁸ S. B. Yang,³⁸ H. Ye,⁸ J. Yelton,⁹ J. H. Yin,²⁶ C. Z. Yuan,²⁶ Y. Yusa,⁶⁶ Z. P. Zhang,⁷⁴ V. Zhilich,^{4, 67} V. Zhukova,⁴³ and V. Zhulanov^{4, 67}

(The Belle Collaboration)

¹University of the Basque Country UPV/EHU, 48080 Bilbao

²Beihang University, Beijing 100191

³Brookhaven National Laboratory, Upton, New York 11973

⁴Budker Institute of Nuclear Physics SB RAS, Novosibirsk 630090

⁵Faculty of Mathematics and Physics, Charles University, 121 16 Prague

⁶Chonnam National University, Kwangju 660-701

⁷University of Cincinnati, Cincinnati, Ohio 45221

⁸Deutsches Elektronen-Synchrotron, 22607 Hamburg

⁹University of Florida, Gainesville, Florida 32611

¹⁰Key Laboratory of Nuclear Physics and Ion-beam Application (MOE) and Institute of Modern Physics, Fudan University, Shanghai 200443

¹¹Justus-Liebig-Universität Gießen, 35392 Gießen

¹²Gifu University, Gifu 501-1193

¹³II. Physikalisches Institut, Georg-August-Universität Göttingen, 37073 Göttingen

¹⁴SOKENDAI (The Graduate University for Advanced Studies), Hayama 240-0193

¹⁵Hanyang University, Seoul 133-791

¹⁶University of Hawaii, Honolulu, Hawaii 96822

¹⁷High Energy Accelerator Research Organization (KEK), Tsukuba 305-0801

¹⁸J-PARC Branch, KEK Theory Center, High Energy Accelerator Research Organization (KEK), Tsukuba 305-0801

¹⁹Forschungszentrum Jülich, 52425 Jülich

²⁰IKERBASQUE, Basque Foundation for Science, 48013 Bilbao

²¹Indian Institute of Science Education and Research Mohali, SAS Nagar, 140306

²²Indian Institute of Technology Guwahati, Assam 781039

²³Indian Institute of Technology Hyderabad, Telangana 502285

²⁴Indian Institute of Technology Madras, Chennai 600036

²⁵Indiana University, Bloomington, Indiana 47408

²⁶Institute of High Energy Physics, Chinese Academy of Sciences, Beijing 100049

²⁷Institute of High Energy Physics, Vienna 1050
²⁸Institute for High Energy Physics, Protvino 142281
²⁹INFN - Sezione di Napoli, 80126 Napoli
³⁰INFN - Sezione di Torino, 10125 Torino
³¹Advanced Science Research Center, Japan Atomic Energy Agency, Naka 319-1195
³²J. Stefan Institute, 1000 Ljubljana
³³Institut für Experimentelle Teilchenphysik, Karlsruher Institut für Technologie, 76131 Karlsruhe
³⁴Kennesaw State University, Kennesaw, Georgia 30144
³⁵Department of Physics, Faculty of Science, King Abdulaziz University, Jeddah 21589
³⁶Kitasato University, Sagamihara 252-0373
³⁷Korea Institute of Science and Technology Information, Daejeon 305-806
³⁸Korea University, Seoul 136-713
³⁹Kyoto University, Kyoto 606-8502
⁴⁰Kyungpook National University, Daegu 702-701
⁴¹LAL, Univ. Paris-Sud, CNRS/IN2P3, Université Paris-Saclay, Orsay
⁴²École Polytechnique Fédérale de Lausanne (EPFL), Lausanne 1015
⁴³P.N. Lebedev Physical Institute of the Russian Academy of Sciences, Moscow 119991
⁴⁴Liaoning Normal University, Dalian 116029
⁴⁵Faculty of Mathematics and Physics, University of Ljubljana, 1000 Ljubljana
⁴⁶Ludwig Maximilians University, 80539 Munich
⁴⁷Luther College, Decorah, Iowa 52101
⁴⁸Malaviya National Institute of Technology Jaipur, Jaipur 302017
⁴⁹University of Malaya, 50603 Kuala Lumpur
⁵⁰University of Maribor, 2000 Maribor
⁵¹Max-Planck-Institut für Physik, 80805 München
⁵²School of Physics, University of Melbourne, Victoria 3010
⁵³University of Mississippi, University, Mississippi 38677
⁵⁴University of Miyazaki, Miyazaki 889-2192
⁵⁵Moscow Physical Engineering Institute, Moscow 115409
⁵⁶Moscow Institute of Physics and Technology, Moscow Region 141700
⁵⁷Graduate School of Science, Nagoya University, Nagoya 464-8602
⁵⁸Kobayashi-Maskawa Institute, Nagoya University, Nagoya 464-8602
⁵⁹Università di Napoli Federico II, 80055 Napoli
⁶⁰Nara Women's University, Nara 630-8506
⁶¹National Central University, Chung-li 32054
⁶²National United University, Miao Li 36003
⁶³Department of Physics, National Taiwan University, Taipei 10617
⁶⁴H. Niewodniczanski Institute of Nuclear Physics, Krakow 31-342
⁶⁵Nippon Dental University, Niigata 951-8580
⁶⁶Niigata University, Niigata 950-2181
⁶⁷Novosibirsk State University, Novosibirsk 630090
⁶⁸Osaka City University, Osaka 558-8585
⁶⁹Pacific Northwest National Laboratory, Richland, Washington 99352
⁷⁰Panjab University, Chandigarh 160014
⁷¹State Key Laboratory of Nuclear Physics and Technology, Peking University, Beijing 100871
⁷²University of Pittsburgh, Pittsburgh, Pennsylvania 15260
⁷³Theoretical Research Division, Nishina Center, RIKEN, Saitama 351-0198
⁷⁴University of Science and Technology of China, Hefei 230026
⁷⁵Seoul National University, Seoul 151-742
⁷⁶Showa Pharmaceutical University, Tokyo 194-8543
⁷⁷Soongsil University, Seoul 156-743
⁷⁸University of South Carolina, Columbia, South Carolina 29208
⁷⁹Stefan Meyer Institute for Subatomic Physics, Vienna 1090
⁸⁰Sungkyunkwan University, Suwon 440-746
⁸¹School of Physics, University of Sydney, New South Wales 2006
⁸²Department of Physics, Faculty of Science, University of Tabuk, Tabuk 71451
⁸³Tata Institute of Fundamental Research, Mumbai 400005
⁸⁴Department of Physics, Technische Universität München, 85748 Garching
⁸⁵Toho University, Funabashi 274-8510
⁸⁶Department of Physics, Tohoku University, Sendai 980-8578
⁸⁷Earthquake Research Institute, University of Tokyo, Tokyo 113-0032
⁸⁸Department of Physics, University of Tokyo, Tokyo 113-0033
⁸⁹Tokyo Institute of Technology, Tokyo 152-8550

⁹⁰*Tokyo Metropolitan University, Tokyo 192-0397*
⁹¹*Virginia Polytechnic Institute and State University, Blacksburg, Virginia 24061*
⁹²*Wayne State University, Detroit, Michigan 48202*
⁹³*Yamagata University, Yamagata 990-8560*
⁹⁴*Yonsei University, Seoul 120-749*

We present the first measurements of the absolute branching fractions of Ξ_c^+ decays into $\Xi^- \pi^+ \pi^+$, $pK^- \pi^+$, and $p\bar{K}^*(892)^0$ final states. Our analysis is based on a data set of $(772 \pm 11) \times 10^6$ $B\bar{B}$ pairs collected at the $\Upsilon(4S)$ resonance with the Belle detector at the KEKB e^+e^- collider. We measure the absolute branching fraction of $\bar{B}^0 \rightarrow \bar{\Lambda}_c^- \Xi_c^+$ with the Ξ_c^+ signal recoiling against $\bar{\Lambda}_c^-$ in \bar{B}^0 decays resulting in $\mathcal{B}(\bar{B}^0 \rightarrow \bar{\Lambda}_c^- \Xi_c^+) = [1.16 \pm 0.42(\text{stat.}) \pm 0.15(\text{syst.})] \times 10^{-3}$. We then measure the product branching fractions $\mathcal{B}(\bar{B}^0 \rightarrow \bar{\Lambda}_c^- \Xi_c^+) \mathcal{B}(\Xi_c^+ \rightarrow \Xi^- \pi^+ \pi^+)$, $\mathcal{B}(\bar{B}^0 \rightarrow \bar{\Lambda}_c^- \Xi_c^+) \mathcal{B}(\Xi_c^+ \rightarrow pK^- \pi^+)$, and $\mathcal{B}(\bar{B}^0 \rightarrow \bar{\Lambda}_c^- \Xi_c^+) \mathcal{B}(\Xi_c^+ \rightarrow p\bar{K}^*(892)^0)$. Dividing these product branching fractions by $\bar{B}^0 \rightarrow \bar{\Lambda}_c^- \Xi_c^+$ yields: $\mathcal{B}(\Xi_c^+ \rightarrow \Xi^- \pi^+ \pi^+) = [2.86 \pm 1.21(\text{stat.}) \pm 0.38(\text{syst.})]\%$, $\mathcal{B}(\Xi_c^+ \rightarrow pK^- \pi^+) = [0.45 \pm 0.21(\text{stat.}) \pm 0.07(\text{syst.})]\%$, and $\mathcal{B}(\Xi_c^+ \rightarrow p\bar{K}^*(892)^0) = [0.25 \pm 0.16(\text{stat.}) \pm 0.04(\text{syst.})]\%$. Our result for $\mathcal{B}(\Xi_c^+ \rightarrow \Xi^- \pi^+ \pi^+)$ can be combined with Ξ_c^+ branching fractions measured relative to $\Xi_c^+ \rightarrow \Xi^- \pi^+ \pi^+$ to set the absolute scale for many Ξ_c^+ branching fractions.

PACS numbers: 14.20.Lq, 13.30.Eg, 13.25.Hw

In recent decades there has been significant experimental progress of the measurements of the weak decays of charmed baryons [1]. However, the large non-perturbative effects of Quantum Chromodynamics make it impossible to reliably calculate the decay amplitudes of charmed baryons from first principles. Furthermore, in exclusive charmed-baryon decays the heavy quark expansion does not work. Hence experimental data are needed to extract the non-perturbative quantities in the decay amplitudes [2–5] and provide important information to constrain phenomenological models of such decays [6–13].

In recent years, Belle and BESIII have measured absolute branching fractions of the Λ_c^+ and Ξ_c^0 charmed baryons [14–16]. However, the absolute branching fraction of the remaining member of the charmed-baryon SU(3) flavor antitriplet, the Ξ_c^+ , has not been measured. Branching fractions of Ξ_c^+ decays have been measured relative to the $\Xi^- \pi^+ \pi^+$ mode. A measurement of the absolute branching fraction $\mathcal{B}(\Xi_c^+ \rightarrow \Xi^- \pi^+ \pi^+)$ is needed to infer the absolute branching fractions of other Ξ_c^+ decays. The comparison of Ξ_c^+ decays with those of Λ_c^+ and Ξ_c^0 can also provide an important test of SU(3) flavor symmetry [17].

A few models have been developed to predict the decay rates of Ξ_c^+ . For example, the $\mathcal{B}(\Xi_c^+ \rightarrow \Xi^- \pi^+ \pi^+)$ has been predicted to be $(1.47 \pm 0.84)\%$ based on the SU(3) flavor symmetry [18]. Experimental information is crucial to not only validate these models, but also to constrain the model parameters.

Along with the reference mode $\Xi_c^+ \rightarrow \Xi^- \pi^+ \pi^+$, $\Xi_c^+ \rightarrow pK^- \pi^+$ is a particularly important decay mode as it is the one most often used to reconstruct Ξ_c^+ candidates at hadron collider experiments, such as LHCb. For example, the decay has been used to study the properties of Ξ_b and to search for higher excited Ξ_b states via $\Xi_b^0 \rightarrow \Xi_c^+ \pi^-$ [19–21], to search for new Ω_c^* states in the $\Xi_c^+ K^-$ mode [22], to measure the doubly charmed

baryon via $\Xi_{cc}^{++} \rightarrow \Xi_c^+ \pi^+$ [23], and to measure the ratio of fragmentation fractions of $b \rightarrow \Xi_b^0$ relative to $b \rightarrow \Lambda_b^0$ [24, 25]. Theory predicts $\mathcal{B}(\Xi_c^+ \rightarrow pK^- \pi^+)$ to be $(2.2 \pm 0.8)\%$ using the measured ratio $\mathcal{B}(\Xi_c^+ \rightarrow p\bar{K}^*)/\mathcal{B}(\Xi_c^+ \rightarrow pK^- \pi^+)$ and the U -spin symmetry that relates $\Xi_c^+ \rightarrow p\bar{K}^*$ and $\Lambda_c^+ \rightarrow \Sigma^+ K^*$ [25, 26]. In experiments, the decay $\Xi_c^+ \rightarrow pK^- \pi^+$ has been observed by the FOCUS and SELEX Collaborations and the branching fraction ratio is measured to be $\mathcal{B}(\Xi_c^+ \rightarrow pK^- \pi^+)/\mathcal{B}(\Xi_c^+ \rightarrow \Xi^- \pi^+ \pi^+) = 0.21 \pm 0.04$ [1, 27–29].

The decay $\bar{B}^0 \rightarrow \bar{\Lambda}_c^- \Xi_c^+$, which proceeds via a $b \rightarrow c\bar{s}$ transition, has been predicted to have a branching fraction of the order 10^{-3} [30], but there has been no experimental measurement. The world average of the product branching fraction $\mathcal{B}(\bar{B}^0 \rightarrow \bar{\Lambda}_c^- \Xi_c^+) \mathcal{B}(\Xi_c^+ \rightarrow \Xi^- \pi^+ \pi^+)$ is $(1.8 \pm 1.8) \times 10^{-5}$ with large uncertainty [1, 31, 32].

In this Letter, we perform an analysis of $\bar{B}^0 \rightarrow \bar{\Lambda}_c^- \Xi_c^+$ with $\bar{\Lambda}_c^-$ reconstructed via its $\bar{p}K^+ \pi^-$ decay, and Ξ_c^+ reconstructed both inclusively and exclusively via the decay modes $\Xi^- \pi^+ \pi^+$, $pK^- \pi^+$, and $p\bar{K}^*(892)^0$ [33]. We present first a measurement of the absolute branching fraction for $\bar{B}^0 \rightarrow \bar{\Lambda}_c^- \Xi_c^+$ using a missing-mass technique. For this analysis we fully reconstruct the tag-side B^0 decay. We subsequently measure the product branching fractions $\mathcal{B}(\bar{B}^0 \rightarrow \bar{\Lambda}_c^- \Xi_c^+) \mathcal{B}(\Xi_c^+ \rightarrow \Xi^- \pi^+ \pi^+)$, $\mathcal{B}(\bar{B}^0 \rightarrow \bar{\Lambda}_c^- \Xi_c^+) \mathcal{B}(\Xi_c^+ \rightarrow pK^- \pi^+)$, and $\mathcal{B}(\bar{B}^0 \rightarrow \bar{\Lambda}_c^- \Xi_c^+) \mathcal{B}(\Xi_c^+ \rightarrow p\bar{K}^*(892)^0)$ without reconstructing the recoiling B^0 decay in the event as the signal decays are fully reconstructed. Dividing these product branching fractions by the result for $\mathcal{B}(\bar{B}^0 \rightarrow \bar{\Lambda}_c^- \Xi_c^+)$ yields the $\mathcal{B}(\Xi_c^+ \rightarrow \Xi^- \pi^+ \pi^+)$, $\mathcal{B}(\Xi_c^+ \rightarrow pK^- \pi^+)$, and $\mathcal{B}(\Xi_c^+ \rightarrow p\bar{K}^*(892)^0)$.

This analysis is based on the full data sample of 711 fb^{-1} collected at the $\Upsilon(4S)$ resonance by the Belle detector [34] at the KEKB asymmetric-energy e^+e^- collider [35].

To determine detection efficiency and optimize signal

event selections, B meson signal events are generated using EVTGEN [36] and Ξ_c^+ inclusive decays are generated using PYTHIA [37]. The events are then processed by a detector simulation based on GEANT3 [38]. Monte Carlo (MC) simulated samples of $\Upsilon(4S) \rightarrow B\bar{B}$ events with $B = B^+$ or B^0 , and $e^+e^- \rightarrow q\bar{q}$ events with $q = u, d, s, c$ at a center-of-mass energy of $\sqrt{s} = 10.58$ GeV are used to examine possible peaking backgrounds.

Selection of signal and $\Lambda \rightarrow p\pi^-$ candidates uses well reconstructed tracks and particle identification as in Ref. [39].

For the inclusive analysis of the Ξ_c^+ decay, the tag-side B^0 meson candidate, B_{tag}^0 , is reconstructed using a neural network based on a full hadron-reconstruction algorithm [40]. Each B_{tag}^0 candidate has an associated output value O_{NN} from the multivariate analysis, which ranges from 0 to 1. A candidate with larger O_{NN} is more likely to be a true B^0 meson. If multiple B_{tag}^0 candidates are found in an event, the candidate with the largest O_{NN} value is selected. To improve the purity of the B_{tag}^0 sample, we require $O_{\text{NN}} > 0.005$, $M_{\text{bc}}^{\text{tag}} > 5.27$ GeV/ c^2 , and $|\Delta E^{\text{tag}}| < 0.04$ GeV, where the latter two intervals correspond to approximately 3 standard deviations, 3σ . $M_{\text{bc}}^{\text{tag}}$ and ΔE^{tag} are defined as $M_{\text{bc}}^{\text{tag}} \equiv \sqrt{E_{\text{beam}}^2 - (\sum_i \vec{p}_i^{\text{tag}})^2}$ and $\Delta E^{\text{tag}} \equiv \sum_i E_i^{\text{tag}} - E_{\text{beam}}$, where $E_{\text{beam}} \equiv \sqrt{s}/2$ is the beam energy, $(E_i^{\text{tag}}, \vec{p}_i^{\text{tag}})$ is the four-momentum of the B_{tag}^0 daughter i in the e^+e^- center-of-mass system (CMS). $\Lambda_c^- \rightarrow \bar{p}K^+\pi^-$ candidates are selected using the same method as in Ref. [16]. A 3σ Λ_c^- signal region is defined by $|M_{\Lambda_c^-} - m_{\Lambda_c^-}| < 10$ MeV/ c^2 . Here and throughout the text, M_i represents a measured invariant mass and m_i represents the nominal mass of the particle i [1].

The mass recoiling against the Λ_c^- in $\bar{B}^0 \rightarrow \bar{\Lambda}_c^- + X$ is calculated using $M_{B_{\text{tag}}^0 \bar{\Lambda}_c^-}^{\text{recoil}} = \sqrt{(P_{\text{CMS}} - P_{B_{\text{tag}}^0} - P_{\bar{\Lambda}_c^-})^2}$. To improve the recoil-mass resolution we use $M_{B_{\text{tag}}^0 \bar{\Lambda}_c^-}^{\text{rec}} \equiv M_{B_{\text{tag}}^0 \bar{\Lambda}_c^-}^{\text{recoil}} + M_{B_{\text{tag}}^0} - m_{B^0} + M_{\bar{\Lambda}_c^-} - m_{\bar{\Lambda}_c^-}$. Here, P_{CMS} , $P_{B_{\text{tag}}^0}$, and $P_{\bar{\Lambda}_c^-}$ are four-momenta of the initial e^+e^- system, the tagged B^0 meson, and the reconstructed $\bar{\Lambda}_c^-$ baryon, respectively.

Figure 1 (left) shows the distribution of $M_{\text{bc}}^{\text{tag}}$ of the B_{tag}^0 candidates versus $M_{\bar{\Lambda}_c^-}$ of the selected $\bar{B}^0 \rightarrow \bar{\Lambda}_c^- \Xi_c^+$ signal candidates after all selection requirements in the studied Ξ_c^+ mass region of $2.4 < M_{B_{\text{tag}}^0 \bar{\Lambda}_c^-}^{\text{rec}} < 2.53$ GeV/ c^2 .

Candidates $\bar{B}^0 \rightarrow \bar{\Lambda}_c^- \Xi_c^+$ are observed in the signal region defined by the solid box. To check possible peaking backgrounds, we define $M_{\text{bc}}^{\text{tag}}$ and $M_{\bar{\Lambda}_c^-}$ sideband regions, which are represented by the dashed and dash-dotted boxes. The normalized contribution of the $M_{\text{bc}}^{\text{tag}}$ and $M_{\bar{\Lambda}_c^-}$ sidebands is estimated as being half the number of events in the blue dashed boxes minus one fourth the number of events in the red dash-dotted boxes. The $M_{B_{\text{tag}}^0 \bar{\Lambda}_c^-}^{\text{rec}}$ distribution in the signal and the sideband

boxes is shown in Figure 1 (right).

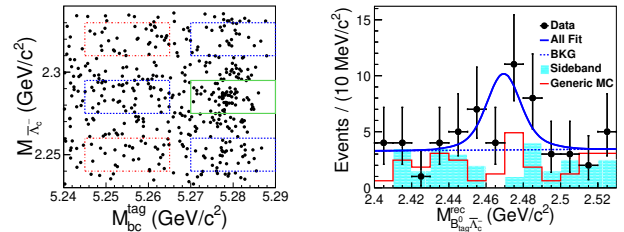


FIG. 1: The distribution of $M_{\text{bc}}^{\text{tag}}$ of the B_{tag}^0 versus $M_{\bar{\Lambda}_c^-}$ for selected $\bar{B}^0 \rightarrow \bar{\Lambda}_c^- \Xi_c^+$ candidates with $\Xi_c^+ \rightarrow \text{anything}$ and $\bar{\Lambda}_c^- \rightarrow \bar{p}K^+\pi^-$ (left) and the fit to the $M_{B_{\text{tag}}^0 \bar{\Lambda}_c^-}^{\text{rec}}$ distribution (right). The solid box shows the selected signal region. The dashed and dash-dotted boxes define the $M_{\text{bc}}^{\text{tag}}$ and $M_{\bar{\Lambda}_c^-}$ sidebands described in the text. The points with error bars are the data in the signal box, the solid blue curve is the best fit, the dashed curve is the fitted background, the cyan shaded histogram is the normalized $M_{\text{bc}}^{\text{tag}}$ and $M_{\bar{\Lambda}_c^-}$ sidebands, the red open histogram is the sum of the MC-simulated contributions for $e^+e^- \rightarrow q\bar{q}$ with $q = u, d, s, c$, and $\Upsilon(4S) \rightarrow B\bar{B}$ generic-decay backgrounds with the number of events normalized to the number of events from the normalized $M_{\text{bc}}^{\text{tag}}$ and $M_{\bar{\Lambda}_c^-}$ sidebands.

To extract the Ξ_c^+ signal yields we perform an unbinned maximum likelihood fit to the $M_{B_{\text{tag}}^0 \bar{\Lambda}_c^-}^{\text{rec}}$ distribution. A double-Gaussian function with its parameters fixed to those from a fit to the MC-simulated signal distribution is used to model the Ξ_c^+ signal shape and a first-order polynomial is used for the background shape since we find no peaking background in the $M_{\text{bc}}^{\text{tag}}$ and $M_{\bar{\Lambda}_c^-}$ sideband events. The fit results are shown in Figure 1 (right).

The fitted number of Ξ_c^+ signal events is $N_{\Xi_c^+} = 18.8 \pm 6.8$. This corresponds to a statistical significance of 3.2σ estimated using $\sqrt{-2 \ln(\mathcal{L}_0/\mathcal{L}_{\text{max}})}$, where \mathcal{L}_0 and \mathcal{L}_{max} are the maximum likelihood values of the fits without and with a signal component, respectively. The branching fraction is

$$\mathcal{B}(\bar{B}^0 \rightarrow \bar{\Lambda}_c^- \Xi_c^+) = N_{\Xi_c^+} / [2N_{\bar{B}^0} \varepsilon_{\text{inc}} \mathcal{B}(\bar{\Lambda}_c^- \rightarrow \bar{p}K^+\pi^-)] \\ = [1.16 \pm 0.42(\text{stat.})] \times 10^{-3},$$

where $N_{\bar{B}^0} = N_{\Upsilon(4S)} \mathcal{B}(\Upsilon(4S) \rightarrow B^0 \bar{B}^0)$, $N_{\Upsilon(4S)}$ is the number of $\Upsilon(4S)$ events, and $\mathcal{B}(\Upsilon(4S) \rightarrow B^0 \bar{B}^0) = 0.486$ [1]. The reconstruction efficiency, ε_{inc} , is obtained from the MC simulation. The $\mathcal{B}(\bar{\Lambda}_c^- \rightarrow \bar{p}K^+\pi^-)$ is taken from Ref. [1].

For the analysis of the exclusive Ξ_c^+ decays, we reconstruct Ξ_c^+ from $\Xi^- \pi^+ \pi^+$ with $\Xi^- \rightarrow \Lambda \pi^-$ ($\Lambda \rightarrow p\pi^-$) and $\Xi^- \rightarrow pK^-\pi^+$ modes, with no B_{tag}^0 . The daughters of the \bar{B}^0 , Ξ_c^+ , and Ξ^- candidates are fit to common vertices. If there is more than one \bar{B}^0 candidate in an event, the one with the smallest $\chi^2_{\text{vertex}}/\text{n.d.f.}$

from the \bar{B}^0 vertex fit is selected. The requirements of $\chi^2_{\text{vertex}}/\text{n.d.f.} < 50$, 15, and 15 are applied to reconstructed \bar{B}^0 , Ξ_c^+ , and Ξ^- candidates, respectively, with selection efficiencies above 96%, 95%, and 95%. Ξ^- and Ξ_c^+ signals are defined as $|M_{\Xi^-} - m_{\Xi^-}| < 10 \text{ MeV}/c^2$ and $|M_{\Xi_c^+} - m_{\Xi_c^+}| < 20 \text{ MeV}/c^2$ corresponding to about 3σ . The $\bar{\Lambda}_c^-$ signal interval is the same as in the inclusive analysis of Ξ_c^+ decays. \bar{B}^0 signal candidates are identified using the beam-constrained mass M_{bc} and the energy difference ΔE . Here, M_{bc} and ΔE are defined as M_{bc}^{tag} and ΔE^{tag} above, but calculated using the momenta of the signal candidate tracks directly.

After the event selections, the distributions of $M_{\Xi_c^+}$ versus $M_{\bar{\Lambda}_c^-}$ in the \bar{B}^0 signal region defined by $|\Delta E| < 0.03 \text{ GeV}$ and $M_{bc} > 5.27 \text{ GeV}/c^2$ corresponding to about 3σ are shown in Figures 2(a1) and 2(a2). The central solid boxes are the Ξ_c^+ and $\bar{\Lambda}_c^-$ signal regions. The backgrounds from non- Ξ_c^+ and non- $\bar{\Lambda}_c^-$ events are estimated with the $M_{\Xi_c^+}$ and $M_{\bar{\Lambda}_c^-}$ sidebands, represented by the dashed and dash-dotted boxes in Figures 2(a1) and 2(a2). The normalized contributions from the $M_{\Xi_c^+}$ and $M_{\bar{\Lambda}_c^-}$ sidebands are estimated using half the number of events in the blue dashed boxes minus one fourth the number of events in the red dash-dotted boxes. Figure 2 shows the M_{bc} and ΔE distributions in the Ξ_c^+ and $\bar{\Lambda}_c^-$ signal regions from the selected $\bar{B}^0 \rightarrow \bar{\Lambda}_c^- \Xi_c^+$ candidates with $\Xi_c^+ \rightarrow \Xi^- \pi^+ \pi^+$ (b1-c1) and $\Xi_c^+ \rightarrow pK^- \pi^+$ (b2-c2) decay modes.

We perform a two-dimensional (2D) maximum-likelihood fit to the M_{bc} and ΔE distributions to extract the number of $\bar{B}^0 \rightarrow \bar{\Lambda}_c^- \Xi_c^+$ signal events with $\Xi_c^+ \rightarrow \Xi^- \pi^+ \pi^+ / pK^- \pi^+$. For the M_{bc} distribution, the signal shape is modeled using a Gaussian function and the background is described using an ARGUS function [41]. For the ΔE distribution, the signal shape is a double-Gaussian and the background is a first-order polynomial. All shape parameters of the signal functions are fixed to the values obtained from the fits to the MC simulated signal distributions. The fit results are shown in Figure 2.

The signal yields are $N_{\Xi^- \pi^+ \pi^+} = 24.2 \pm 5.4$ (6.9σ significance) and $N_{pK^- \pi^+} = 24.0 \pm 6.9$ (4.5σ significance). We use the efficiencies from MC simulations to measure $\mathcal{B}(\bar{B}^0 \rightarrow \bar{\Lambda}_c^- \Xi_c^+) \mathcal{B}(\Xi_c^+ \rightarrow \Xi^- \pi^+ \pi^+)$ and $\mathcal{B}(\bar{B}^0 \rightarrow \bar{\Lambda}_c^- \Xi_c^+) \mathcal{B}(\Xi_c^+ \rightarrow pK^- \pi^+)$ as $[3.32 \pm 0.74(\text{stat.})] \times 10^{-5}$ and $[5.27 \pm 1.51(\text{stat.})] \times 10^{-6}$, respectively.

To extract the $\Xi_c^+ \rightarrow p\bar{K}^*(892)^0 \rightarrow pK^- \pi^+$ signal yields, we do an unbinned, three-dimensional, maximum-likelihood fit to the $M_{K^- \pi^+}$, M_{bc} , and ΔE distributions. For the M_{bc} and ΔE distributions, the same fitting functions are taken as in the 2D fit for the signal and background events described above. For the $M_{K^- \pi^+}$ distribution, the signal shape is a P -wave relativistic Breit-Wigner (RBW) function with shape parameters fixed to the values obtained from fitting the MC simulated distribution, and the background shape is a

first-order polynomial plus an additional P -wave RBW for a possible peaking background contribution with a $\bar{K}^*(892)^0$ signal. We show the fit results in Figures 2(d-f). The fitted signal yield is $N_{p\bar{K}^*(892)^0} = 8.9 \pm 3.9$ (3.3σ significance). The measured $\mathcal{B}(\bar{B}^0 \rightarrow \bar{\Lambda}_c^- \Xi_c^+) \mathcal{B}(\Xi_c^+ \rightarrow p\bar{K}^*(892)^0)$ is $[2.96 \pm 1.31(\text{stat.})] \times 10^{-6}$.

We divide the above product branching fractions by the value of $\mathcal{B}(\bar{B}^0 \rightarrow \bar{\Lambda}_c^- \Xi_c^+)$ and for the first time measure $\mathcal{B}(\Xi_c^+ \rightarrow \Xi^- \pi^+ \pi^+)$, $\mathcal{B}(\Xi_c^+ \rightarrow pK^- \pi^+)$, $\mathcal{B}(\Xi_c^+ \rightarrow p\bar{K}^*(892)^0)$, and the ratios between them. These are shown in Table I.

There are several sources of systematic uncertainties in the branching fraction measurements. The uncertainties related to reconstruction efficiency include those for tracking efficiency (0.35% per track), particle identification efficiency (0.9% per kaon, 0.9% per pion, and 3.3% per proton), as well as Λ reconstruction efficiency (3.0% per Λ [42]). We assume these reconstruction-efficiency-related uncertainties are independent and sum them in quadrature. We estimate the systematic uncertainties associated with the fitting procedures by changing the order of the background polynomial, the range of the fit, and by enlarging the mass resolution by 10%. The observed deviations from the nominal fit results are taken as systematic uncertainties. The uncertainty on $\mathcal{B}(\bar{\Lambda}_c^- \rightarrow \bar{p}K^+ \pi^-)$ is taken from Ref. [1]. The uncertainty due to the B^0 tagging efficiency is 4.5% [43]. A relative systematic uncertainty on $\mathcal{B}(\Upsilon(4S) \rightarrow B^0 \bar{B}^0)$ is 1.23% [1]. The systematic uncertainty on $N_{\Upsilon(4S)}$ is 1.37% [44]. For the Ξ_c^+ branching fractions and the corresponding ratios, some common systematic uncertainties, including tracking, particle identification, $\bar{\Lambda}_c^-$ decay branching fraction, Λ selection, and the total number of $B\bar{B}$ pairs, cancel. We summarize the sources of systematic uncertainties in Table I, assume them to be independent, and add them in quadrature to obtain the total systematic uncertainties.

We report the first measurements of the absolute branching fractions

$$\mathcal{B}(\Xi_c^+ \rightarrow \Xi^- \pi^+ \pi^+) = (2.86 \pm 1.21 \pm 0.38)\%,$$

$$\mathcal{B}(\Xi_c^+ \rightarrow pK^- \pi^+) = (0.45 \pm 0.21 \pm 0.07)\%,$$

$$\mathcal{B}(\Xi_c^+ \rightarrow p\bar{K}^*(892)^0) = (0.25 \pm 0.16 \pm 0.04)\%,$$

where the first uncertainties are statistical and the second systematic. The measured $\mathcal{B}(\Xi_c^+ \rightarrow \Xi^- \pi^+ \pi^+)$ value is consistent with the theoretical prediction within uncertainties [18]. The measured central value of $\mathcal{B}(\Xi_c^+ \rightarrow pK^- \pi^+)$ is smaller than that of the theoretical prediction [25, 26], perhaps indicating a large U -spin symmetry breaking effect in the singly-Cabibbo-suppressed charmed-baryon decays. The branching fraction $\mathcal{B}(\bar{B}^0 \rightarrow \bar{\Lambda}_c^- \Xi_c^+)$ is measured for the first time to be $[1.16 \pm 0.42(\text{stat.}) \pm 0.15(\text{syst.})] \times 10^{-3}$ and agrees well with that of $B^- \rightarrow \bar{\Lambda}_c^- \Xi_c^0$ [16] agreeing with

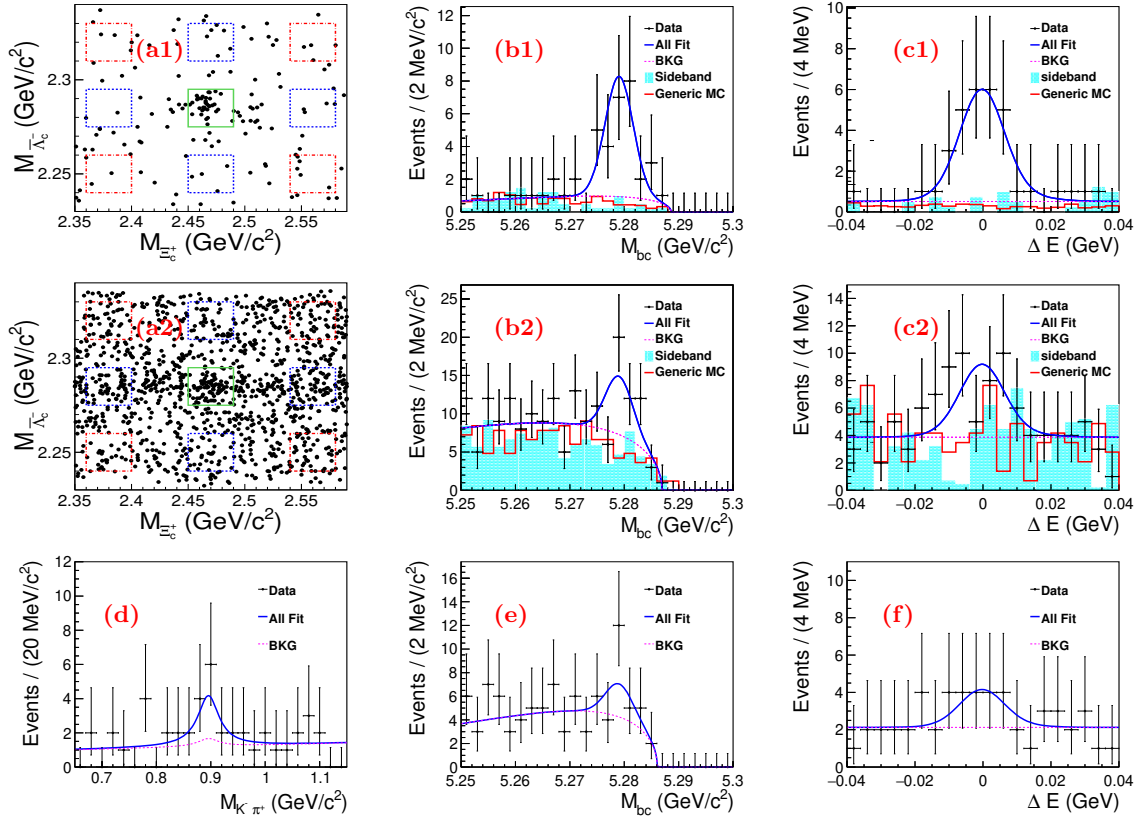


FIG. 2: The distributions of (a) $M_{\Xi_c^+}$ versus $M_{\bar{\Lambda}_c^-}$, and the fits to the (b) M_{bc} and (c) ΔE distributions of the selected $\bar{B}^0 \rightarrow \bar{\Lambda}_c^- \Xi_c^+$ candidates for (b1-c1) the $\Xi_c^+ \rightarrow \Xi^- \pi^+ \pi^+$ and (b2-c2) the $\Xi_c^+ \rightarrow pK^- \pi^+$ decay modes. Plots (d-f) show the fit to (d) the $M_{K^- \pi^+}$, (e) the M_{bc} , and (f) the ΔE distributions for the $\Xi_c^+ \rightarrow p\bar{K}^*(892)^0 \rightarrow pK^- \pi^+$ decay mode. In plots (a1-a2), the central solid boxes are the signal regions, and the red dash-dotted and blue dashed boxes show the $M_{\Xi_c^+}$ and $M_{\bar{\Lambda}_c^-}$ sideband regions used to estimate of the backgrounds (see text). The dots with error bars are the data, the blue solid curves represent the best fits, and the dashed curves represent the fit background contributions. The shaded histograms are the normalized as in the text $M_{\Xi_c^+}$ and $M_{\bar{\Lambda}_c^-}$ sidebands, the red open histograms are from the sum of the MC-simulated contributions from the $e^+ e^- \rightarrow q\bar{q}$ with $q = u, d, s, c$, and $\Upsilon(4S) \rightarrow B\bar{B}$ generic-decay backgrounds with the number of events normalized to the number of events from the normalized $M_{\Xi_c^+}$ and $M_{\bar{\Lambda}_c^-}$ sidebands.

TABLE I: Summary of the measured Ξ_c^+ branching fractions and ratios (last column), and the corresponding systematic uncertainties in %. For the branching fractions and ratios, the first uncertainties are statistical and the second are systematic.

Observable	Efficiency	Fit	Λ_c decays	B_{tag}	$N_{\bar{B}^0}$	Sum	Measured value
$\mathcal{B}(\bar{B}^0 \rightarrow \bar{\Lambda}_c^- \Xi_c^+)$	3.66	10.3	5.3	4.5	1.82	13.1	$(1.16 \pm 0.42 \pm 0.15) \times 10^{-3}$
$\mathcal{B}(\bar{B}^0 \rightarrow \bar{\Lambda}_c^- \Xi_c^+) \mathcal{B}(\Xi_c^+ \rightarrow \Xi^- \pi^+ \pi^+)$	6.24	5.61	5.3	...	1.82	10.1	$(3.32 \pm 0.74 \pm 0.33) \times 10^{-5}$
$\mathcal{B}(\bar{B}^0 \rightarrow \bar{\Lambda}_c^- \Xi_c^+) \mathcal{B}(\Xi_c^+ \rightarrow pK^- \pi^+)$	7.32	9.53	5.3	...	1.82	13.3	$(5.27 \pm 1.51 \pm 0.69) \times 10^{-6}$
$\mathcal{B}(\bar{B}^0 \rightarrow \bar{\Lambda}_c^- \Xi_c^+) \mathcal{B}(\Xi_c^+ \rightarrow p\bar{K}^*(892)^0)$	7.32	11.5	5.3	...	1.82	14.7	$(2.96 \pm 1.31 \pm 0.44) \times 10^{-6}$
$\mathcal{B}(\Xi_c^+ \rightarrow \Xi^- \pi^+ \pi^+)$	4.23	11.7	...	4.5	...	13.2	$(2.86 \pm 1.21 \pm 0.38)\%$
$\mathcal{B}(\Xi_c^+ \rightarrow pK^- \pi^+)$	3.66	14.0	...	4.5	...	15.2	$(0.45 \pm 0.21 \pm 0.07)\%$
$\mathcal{B}(\Xi_c^+ \rightarrow p\bar{K}^*(892)^0)$	3.66	15.4	...	4.5	...	16.5	$(0.25 \pm 0.16 \pm 0.04)\%$
$\mathcal{B}(\Xi_c^+ \rightarrow pK^- \pi^+) / \mathcal{B}(\Xi_c^+ \rightarrow \Xi^- \pi^+ \pi^+)$	4.90	11.0	12.0	$0.16 \pm 0.06 \pm 0.02$
$\mathcal{B}(\Xi_c^+ \rightarrow p\bar{K}^*(892)^0) / \mathcal{B}(\Xi_c^+ \rightarrow \Xi^- \pi^+ \pi^+)$	4.90	12.8	13.7	$0.09 \pm 0.04 \pm 0.01$
$\mathcal{B}(\Xi_c^+ \rightarrow p\bar{K}^*(892)^0) / \mathcal{B}(\Xi_c^+ \rightarrow pK^- \pi^+)$...	14.9	14.9	$0.56 \pm 0.30 \pm 0.08$

the expectation from isospin symmetry. The product branching fractions are

$$\begin{aligned} & \mathcal{B}(\bar{B}^0 \rightarrow \bar{\Lambda}_c^-\Xi_c^+) \mathcal{B}(\Xi_c^+ \rightarrow \Xi^-\pi^+\pi^+) \\ &= [3.32 \pm 0.74(\text{stat.}) \pm 0.33(\text{stat.})] \times 10^{-5}, \\ & \mathcal{B}(\bar{B}^0 \rightarrow \bar{\Lambda}_c^-\Xi_c^+) \mathcal{B}(\Xi_c^+ \rightarrow pK^-\pi^+) \\ &= [5.27 \pm 1.51(\text{stat.}) \pm 0.69(\text{syst.})] \times 10^{-6}, \\ & \mathcal{B}(\bar{B}^0 \rightarrow \bar{\Lambda}_c^-\Xi_c^+) \mathcal{B}(\Xi_c^+ \rightarrow p\bar{K}^*(892)^0) \\ &= [2.96 \pm 1.31(\text{stat.}) \pm 0.44(\text{syst.})] \times 10^{-6}. \end{aligned}$$

The first of these branching fraction measurements is consistent with previous measurements, with improved precision, and supersedes the Belle measurement [31]. The ratios $\mathcal{B}(\Xi_c^+ \rightarrow pK^-\pi^+)/\mathcal{B}(\Xi_c^+ \rightarrow \Xi^-\pi^+\pi^+)$, $\mathcal{B}(\Xi_c^+ \rightarrow p\bar{K}^*(892)^0)/\mathcal{B}(\Xi_c^+ \rightarrow \Xi^-\pi^+\pi^+)$, and $\mathcal{B}(\Xi_c^+ \rightarrow p\bar{K}^*(892)^0)/\mathcal{B}(\Xi_c^+ \rightarrow pK^-\pi^+)$ are measured to be $0.16 \pm 0.06(\text{stat.}) \pm 0.02(\text{syst.})$, $0.09 \pm 0.04(\text{stat.}) \pm 0.01(\text{syst.})$, and $0.56 \pm 0.30(\text{stat.}) \pm 0.08(\text{syst.})$, respectively, which are consistent with world-average values of 0.21 ± 0.04 , 0.12 ± 0.03 , and 0.54 ± 0.11 [1] within uncertainties. Our measured Ξ_c^+ branching fractions, e.g. for $\Xi_c^+ \rightarrow \Xi^-\pi^+\pi^+$, can be combined with Ξ_c^+ branching fractions measured relative to $\Xi_c^+ \rightarrow \Xi^-\pi^+\pi^+$ to yield other absolute Ξ_c^+ branching fractions.

In summary, based on $(772 \pm 11) \times 10^6$ $B\bar{B}$ pairs collected at the $\Upsilon(4S)$ resonance with the Belle detector, we perform an analysis of $\bar{B}^0 \rightarrow \bar{\Lambda}_c^-\Xi_c^+$ inclusively using a hadronic B -tagging method based on a full reconstruction algorithm [40], and exclusively with Ξ_c^+ decays into $\Xi^-\pi^+\pi^+$, $pK^-\pi^+$, and $p\bar{K}^*(892)^0$ final states. These are the first measures of the absolute branching fractions $\mathcal{B}(\Xi_c^+ \rightarrow \Xi^-\pi^+\pi^+)$, $\mathcal{B}(\Xi_c^+ \rightarrow pK^-\pi^+)$, and $\mathcal{B}(\Xi_c^+ \rightarrow p\bar{K}^*(892)^0)$.

We thank Professor Fu-sheng Yu for useful discussions and comments. We thank the KEKB group for excellent operation of the accelerator; the KEK cryogenics group for efficient solenoid operations; and the KEK computer group, the NII, and PNNL/EMSL for valuable computing and SINET5 network support. We acknowledge support from MEXT, JSPS and Nagoya's TLPRC (Japan); ARC (Australia); FWF (Austria); NSFC and CCEPP (China); MSMT (Czechia); CZF, DFG, EXC153, and VS (Germany); DST (India); INFN (Italy); MOE, MSIP, NRF, RSRI, FLRFAS project and GSDC of KISTI and KREONET/GLORIAD (Korea); MNiSW and NCN (Poland); MSHE (Russia); ARRS (Slovenia); IKERBASQUE (Spain); SNSF (Switzerland); MOE and MOST (Taiwan); and DOE and NSF (USA).

- [3] H. Y. Cheng and C. W. Chiang, Phys. Rev. D **81**, 074021 (2010).
- [4] H. N. Li, C. D. Lü, and F. S. Yu, Phys. Rev. D **86**, 036012 (2012).
- [5] S. Müller, U. Nierste, and S. Schacht, Phys. Rev. D **92**, 014004 (2015).
- [6] J. G. Körner, G. Krämer, and J. Wilrodt, Z. Phys. C **2**, 117 (1979).
- [7] T. Uppal, R. C. Verma, and M. P. Khanna, Phys. Rev. D **49**, 3417 (1994).
- [8] G. Kaur and M. P. Khanna, Phys. Rev. D **44**, 182 (1991).
- [9] Q. P. Xu and A. N. Kamal, Phys. Rev. D **46**, 270 (1992).
- [10] P. Zencykowski, Phys. Rev. D **50**, 402 (1994).
- [11] J. G. Körner and G. Krämer, Z. Phys. C **55**, 659 (1992).
- [12] H. Y. Cheng and B. Tseng, Phys. Rev. D **46**, 1042 (1992) [Erratum: Phys. Rev. D **55**, 1697 (1997)].
- [13] H. Y. Cheng and B. Tseng, Phys. Rev. D **48**, 4188 (1993).
- [14] A. Zupanc *et al.* (Belle Collaboration), Phys. Rev. Lett. **113**, 042002 (2014).
- [15] M. Ablikim *et al.* (BESIII Collaboration), Phys. Rev. Lett. **116**, 052001 (2016).
- [16] Y. B. Li *et al.* (Belle Collaboration), Phys. Rev. Lett. **122**, 082001 (2019).
- [17] M. J. Savage and R. P. Springer, Phys. Rev. D **42**, 1527 (1990).
- [18] C. Q. Geng, Y.K. Hsiao, C. W. Liu, and T. H. Tsai, Phys. Rev. D **97**, 073006 (2018).
- [19] R. Aaij *et al.* (LHCb Collaboration), Phys. Rev. Lett. **121**, 162002 (2018).
- [20] R. Aaij *et al.* (LHCb Collaboration), Phys. Rev. D **121**, 072002 (2018).
- [21] R. Aaij *et al.* (LHCb Collaboration), Phys. Rev. D **121**, 072002 (2018).
- [22] R. Aaij *et al.* (LHCb Collaboration), Phys. Rev. Lett. **118**, 182001 (2017).
- [23] R. Aaij *et al.* (LHCb Collaboration), Phys. Rev. Lett. **121**, 162002 (2018).
- [24] R. Aaij *et al.* (LHCb Collaboration), Phys. Rev. Lett. **113**, 032001 (2014).
- [25] H. Y. Jiang and F. S. Yu, Eur. Phys. J. C **78**, 224 (2018).
- [26] F. S. Yu, H. Y. Jiang, R. H. Li, C. D. Lü, W. Wang, and Z. X. Zhao, Chin. Phys. C **42**, 051001 (2018).
- [27] S. Y. Jun *et al.* (SELEX Collaboration), Phys. Rev. Lett. **84**, 1857 (2000).
- [28] J. M. Link *et al.* (FOCUS Collaboration), Phys. Lett. B **512**, 277 (2001).
- [29] E. Vazquez-Jauregui *et al.* (SELEX Collaboration), Phys. Lett. B **666**, 299 (2008).
- [30] H. Y. Cheng, C. K. Chua, and S. Y. Tsai, Phys. Rev. D **73**, 074015 (2006).
- [31] R. Chistov *et al.* (Belle Collaboration), Phys. Rev. D **74**, 111105 (2006).
- [32] B. Aubert *et al.* (BABAR Collaboration), Phys. Rev. D **77**, 031101 (2008).
- [33] Inclusion of charge-conjugate states is implicit unless otherwise stated.
- [34] A. Abashian *et al.* (Belle Collaboration), Nucl. Instrum. Methods Phys. Res., Sect. A **479**, 117 (2002); also, see detector section in J. Brodzicka *et al.*, Prog. Theor. Exp. Phys. (2012) 04D001.
- [35] S. Kurokawa and E. Kikutani, Nucl. Instrum. Methods Phys. Res., Sect. A **499**, 1 (2003), and other papers included in this volume; T. Abe *et al.*, Prog. Theor. Exp. Phys. (2013) 03A001 and following articles up to 03A011.

- [1] M. Tanabashi *et al.* (Particle Data Group), Phys. Rev. D **98**, 030001 (2018).
- [2] B. Bhattacharya and J. L. Rosner, Phys. Rev. D **77**, 114020 (2008).

- [36] D. J. Lange, Nucl. Instrum. Methods Phys. Res., Sect. A **462**, 152 (2001).
- [37] T. Sjöstrand *et al.*, Comput. Phys. Commun. **135**, 238 (2001).
- [38] R. Brun *et al.*, GEANT, CERN Report No. DD/EE/84-1 (1984).
- [39] Y. B. Li *et al.* (Belle Collaboration), Eur. Phys. J. C **78**, 928 (2018).
- [40] M. Feindt, F. Keller, M. Kreps, T. Kuhr, S. Neubauer, D. Zander, and A. Zupanc, Nucl. Instrum. Methods Phys. Res., Sect. A **654**, 432 (2011).
- [41] H. Albrecht *et al.* (ARGUS Collaboration), Phys. Lett. B **229**, 304 (1989).
- [42] Y. Kato *et al.* (Belle Collaboration), Phys. Rev. D **94**, 032002 (2016).
- [43] A. Sibidanov *et al.* (Belle Collaboration), Phys. Rev. D **88**, 032005 (2013).
- [44] E. Guido *et al.* (Belle Collaboration), Phys. Rev. D **96**, 052005 (2017).